Full Length Research Paper

Melting and radiation effects on mixed convection from a vertical surface embedded in a non-Newtonian fluid saturated non-Darcy porous medium for aiding and opposing eternal flows

Ali J. Chamkha[1]*, Sameh E. Ahmed[2] and Abdulkareem S. Aloraier[1]

[1]Manufacturing Engineering Department, The Public Authority for Applied Education and Training, Shuweikh 70654, Kuwait.
[2]Department of Mathematics, South Valley University, Qena, Egypt.

Continuum equations governing mixed convection from a vertical surface embedded in a non-Darcy porous medium with aiding and opposing external flows in the presence of melting, radiation and heat generation or absorption effects for non-Newtonian fluids are developed. Similarity variables are employed for the partial differential equations governing the flow and heat transfer characteristics and the resulting ordinary differential equations are solved numerically by an implicit, iterative, finite-difference method. The accuracy of the numerical method is tested by performing various comparisons with previously published work and the results are found to be in excellent agreement. Representative Flow and heat transfer results are obtained for various combinations of physical parameters. These results are presented graphically to illustrate interesting features of the physics of the problem.

Key words: Melting effect, non-Newtonian fluid, non-Darcy flow, thermal radiation, heat generation or absorption.

INTRODUCTION

Convection heat transfer in porous media in the presence of melting effect has received some attention in recent years. This stems from the fact that this topic has significant direct application in permafrost melting, frozen ground thawing, casting and welding processes as well as phase change material (PCM). This has shown to be of special interest in the permafrost research in which the melting effect plays an important role in problems of permafrost melting and frozen ground thawing (Cheng and Lin, 2008). According to the analysis of Walker (2007), the phenomenon of permafrost degradation in Arctic Alaska is very critical due to global warming and this result accelerates the greenhouse effect. Many studies have been reported to study the melting process by heat convection mechanism under steady state (Gorla et al., 1999; Bakier, 1997; Cheng and Lin, 2007; Tashtoush, 2005; Bakier et al., 2009) or unsteady state (Zhang and Bejan, 1989; Chang and Yang, 1996; Cheng and Lin, 2006) conditions to provide understanding of the melting phenomenon.

As mentioned before, the study of melting effect is considered by many previous authors. For example, Roberts (1958) firstly presented "shielding effect" to describe the melting phenomena of ice placed in a hot stream of air at a steady state. Later, from the point of view of boundary layer theory, film theory and penetration theory, Tien and Yen (1965) studied the effect of melting on convective heat transfer between a melting body and surrounding fluid. Epstein and Cho (1976) considered the laminar film condensation on a vertical melting surface for 1-D and 2-D systems based on Nusselt's method to discuss the melting rate. They pointed out that as long as the melting solid is large compared with the thickness of thermal boundary layer, transient effects in the solid would be neglected. Sparrow et al. (1977) studied the velocity and temperature fields, the heat transfer rate and the melting layer thickness by means of a finite-difference scheme in the melting region for natural convection.

---

*Corresponding author. E-mail: achamkha@yahoo.com.

The non-linear behavior of non-Newtonian fluids in a porous matrix is quite different from that of Newtonian fluids in porous media. The prediction of heat or mass transfer characteristics for mixed or natural convection of non-Newtonian fluids in porous media is very important due to its practical engineering applications, such as oil recovery and food processing. Kumaria and Nath (2006) studied the conjugate mixed convection conduction heat transfer of a non-Newtonian power- law fluid on a vertical heated plate which is moving in an ambient fluid. Degan et al. (2007) presented an analytical method to investigate transient free convection boundary layer flow along a vertical surface embedded in an anisotropic porous medium saturated by a non-Newtonian fluid. The problem of double-diffusive natural convection near a vertical wavy truncated cone in a non-Newtonian fluid saturated porous medium with thermal and mass stratification was presented by Cheng (2008). Poulikakos and Spatz (1988) investigated the effect of non-Newtonian natural convection at a melting front in a permeable matrix. Their results documented the dependence of the local heat transfer rate at the melting front on the type of power-law fluid saturating the porous matrix. Recently, Rastogi and Poulikakos (1995) studied the double diffusion from a vertical surface embedded in a porous medium saturated by a non-Newtonian fluid. These authors have found that the variation of the wall temperature and concentration necessary to yield a constant heat and species flux at the wall depended strongly on the power-law fluid index.

Due to the important and interesting applications in geothermal energy extraction, nuclear waste disposal industry, underground heat exchangers for energy storage and recovery, temperature controlled reactors, packed beds and the utilization of porous layers for transpiration cooling by water for fire fighting, in the storage of food grains, and also in resin transfer molding process in which fiber reinforced polymeric parts are produced in final shape, etc., the study of convective heat transfer in a non-Darcy porous medium has been gaining the attention of several researchers. Chamkha (1996) presented a numerical study for non-Darcy hydromagnetic free convection flow of an electrically-conducting and heat-generating fluid over a vertical cone and a wedge adjacent to a porous medium. Murthy and Singh (2000) investigated the effect of viscous dissipation on non-Darcy natural convection flow along an isothermal vertical wall embedded in a saturated porous medium. Afify (2007) performed an analysis for non-Darcy free convection flow of an electrically-conducting fluid over an impermeable vertical plate embedded in a thermally stratified, fluid-saturated porous medium for the case of power-law surface temperature.

In problems dealing with porous media, the effects of melting, radiation and heat generation or absorption become important (Gorla et al., 1999; Cheng and Lin, 2007; Kazmierczak et al., 1987; Kazmierczak et al., 1986;

Chen et al., 1986). The problem of unsteady mixed convection boundary layer flow near the stagnation point on a heated vertical plate embedded in a fluid saturated porous medium with thermal radiation and variable viscosity was investigated by Hassanien and Al-arabi (2009). Murthy et al. (2004) considered mixed convection flow of an absorbing fluid up a uniform non–Darcy porous medium supported by a semi-infinite ideally transparent vertical flat plate due to solar radiation. Chamkha et al. (2006) presented a numerical study of coupled heat and mass transfer by boundary-layer free convection over a vertical flat plate embedded in a fluid-saturated porous medium in the presence of thermophoretic particle deposition and heat generation or absorption effects. Ali (2007) discussed the effect of suction or injection on the free convection boundary layers induced by a heated vertical plate embedded in a saturated porous medium with an exponential decaying heat generation.

Motivated by the works mentioned above, the main objective of this work is to study the effects of melting, thermal radiation and heat generation or absorption on steady mixed convection from a vertical wall embedded in a non-Newtonian power-law fluid saturated non-Darcy porous medium for aiding and opposing external flows. Similarity transformations are used to obtain self-similar equations which are solved numerically using the finite-difference method.

GOVERNING EQUATIONS

Consider steady mixed convection along a vertical flat plate immersed in a non-Newtonian fluid saturated porous medium with aiding and opposing external flows in the presence of melting, radiation and heat generation or absorption effects. The schematic of the problem and coordinate system are shown in Figure 1. In the present problem, the following assumptions are made:

(1) A uniform source of heat generation or absorption in the flow region with constant volumetric rate is considered.
(2) Properties of the fluid are isotropic and homogeneous everywhere.
(3) Thermal radiation effect with Rosseland approximation is considered.
(4) The Boussinesq approximation is employed.
(5) The viscous dissipation effect is neglected.
(6) The two-phase system is in local thermal equilibrium with the porous medium.
(7) The free stream temperature of the fluid is taken as a constant $T_\infty \, (T_\infty > T_m)$.
(8) The free stream temperature of the solid phase is taken as a constant $T_s \, (T_s < T_m)$.

Under these assumptions the continuity, momentum and energy equations are given by:
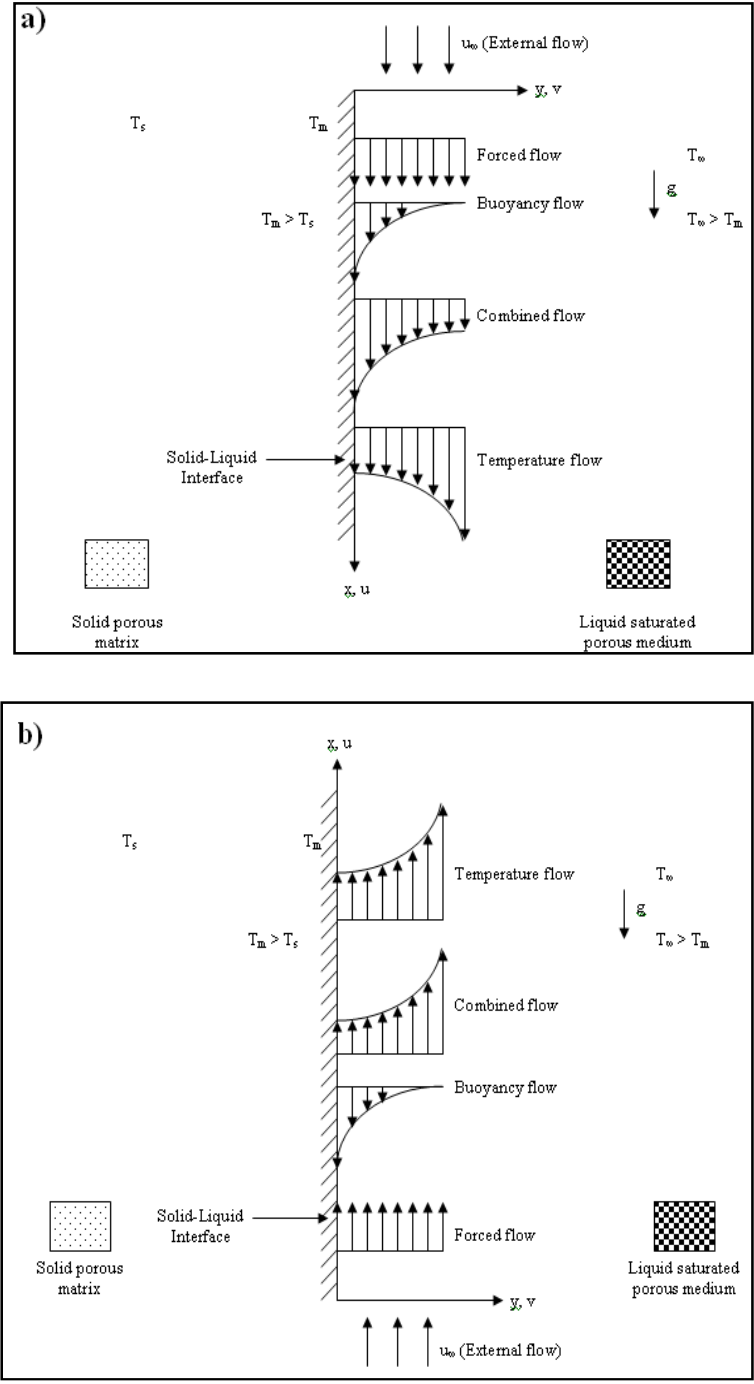
Figure 1. Schematic diagram and coordinate system: (a) aiding external flow and (b) opposing external flow.

$$\frac{\partial u}{\partial x} + \frac{\partial v}{\partial y} = 0,$$ (1)

$$\frac{\partial u^n}{\partial y} + \frac{c\sqrt{K}}{v}\frac{\partial u^2}{\partial y} = \mp\frac{Kg\beta}{v}\frac{\partial T}{\partial y},$$ (2)

$$u\frac{\partial T}{\partial x} + v\frac{\partial T}{\partial y} = \alpha\left[\frac{\partial^2 T}{\partial y^2} - \frac{1}{k_{eff}}\frac{\partial q^r}{\partial y}\right] + \frac{\alpha Q_0}{k_{eff}}(T - T_m),$$ (3)

In the above equations, the term which represents the buoyancy forced effect on the flow field, has $\pm$ signs; the plus sign indicates buoyancy-assisted flow whereas the

negative sign stands for buoyancy-opposed flow and u and v are Darcy's velocity in the x and y directions; K is the permeability constant, c is an Forchheimer empirical constant, T is temperature in thermal boundary layer; $\upsilon = \mu / \rho_\infty$ is modified kinematic viscosity; $\alpha = k_{eff} /(\rho_\infty c_{pf})$ is the equivalent thermal diffusivity with denoting the product of density ρ_∞ and specific heat (c_{pf}) of the convective fluid, and k_{eff} the effective thermal conductivity of the saturated porous medium given by

$$k_{eff} = (1-\varepsilon)k_s + \varepsilon k_f,$$

where ε, k_s and k_f are the porosity of the medium, thermal conductivity of the solid and convective fluid, respectively. n, g, T_m, q^r and Q_0 are the power-law fluid viscosity index, acceleration due to gravity, melting temperature, radiative heat flux and volumetric heat generation or absorption parameter, respectively.

The physical boundary conditions for the present problem are

$$y = 0, \ T = T_m, \ k_{eff} \frac{\partial T}{\partial y} = \rho_f[\lambda + C_s(T_m - T_s)]v, \tag{4}$$

$$y \rightarrow \infty, \ T = T_\infty, \ u = u_\infty.$$

where ρ_f, λ, C_s and u_∞ are density of convective fluid, latent heat of melting of solid, specific heat of solid phase and free stream velocity, respectively.

With the assumption of Rosseland approximation, the radiative heat flux q^r can be written as:

$$q^r = -\frac{4\sigma}{3K_0} \frac{\partial T^4}{\partial y}, \tag{5}$$

where σ is the Stefan-Boltzmann constant and K_0 is the mean absorption coefficient.

If temperature differences within the flow are sufficiently small such that T^4 may be expressed as a linear function of the temperature, then the Taylor series expansion for T^4 about T_m, after neglecting higher order terms, can be written as

$$T^4 \approx 4TT_m^3 - 3T_m^4. \tag{6}$$

In view of equations (5) and (6), equation (3) reduces to

$$u \frac{\partial T}{\partial x} + v \frac{\partial T}{\partial y} = \alpha \left(1 + \frac{16\sigma T_m^3}{3k_{eff} K_0}\right)\frac{\partial^2 T}{\partial y^2} + \frac{\alpha Q_0}{k_{eff}}(T - T_m) \tag{7}$$

To get the self-similar form for the forced convection-dominated regime, we will consider the following transformation:

$$\eta = \frac{y}{x} Pe_x^{1/2}, \ \psi = \alpha Pe_x^{1/2} f(\eta), \ Pe_x = \frac{u_\infty x}{\alpha}, \ \Omega = \frac{Ra_x}{Pe_x},$$

$$Ra_x = \left(\frac{xg\beta k_{eff}\Delta T}{\alpha \upsilon}\right)^{1/n}, \ \theta = \frac{T - T_m}{\Delta T}, \ \Delta T = T_\infty - T_m \tag{8}$$

Substituting equation (8) into equations (2) and (7), we get the following similarity equations:

$$nf''f'^{n-1} + 2\text{Re}_d \ ff'' = \mp\Omega\theta', \tag{9}$$

$$\theta''\left(1 + \frac{4R_d}{3}\right) + \theta' \frac{f}{2} + \gamma\theta = 0 \tag{10}$$

where the primes in the equations indicate ordinary differentiation with respect to η, f is the dimensionless stream function, θ is the dimensionless temperature, Ω is the buoyancy parameter, $R_d = 4\sigma T_m^3 / k_{eff} K_0$ is the radiation parameter, $\text{Re}_d = u_\infty^n d / \upsilon$ is the pore diameter dependent Reynolds number and $\gamma = Q_0 x^2 / k_{eff} Pe_x$ is the dimensionless heat generation or absorption parameter.

The transformed dimensionless boundary conditions are:

$$\eta = 0 : \theta = 0, \ f + 2M\theta' = 0,$$
$$\eta \rightarrow \infty, \ \theta = 1.0, \ f' = 1.0 \tag{11}$$

where $M = c_{pf}\Delta T /(\lambda + C_s(T_m - T_s))$ is the melting parameter combining Stefan numbers $c_{pf}\Delta T / \lambda$ and $C_s(T_m - T_s)/\lambda$ for the liquid and solid phases, respectively. In addition, the velocity components in x and y directions can be written as:

$$u = \frac{\alpha Pe_x}{x} f', \ v = \frac{-\alpha Pe_x^{1/2}}{x}\left[\frac{f}{2} - \frac{\eta}{2} f'\right]. \tag{12}$$

Physical quantities of interest are the skin-friction coefficient C_f and the Nusselt number Nu_x which are defined as

$$C_f = \frac{\tau_w}{\rho u_\infty^2 / 2}, \ Nu_x = \frac{xq_w}{k_{eff}\Delta T}, . \tag{13}$$

Further, τ_w and q_w are the shear stress and the heat transfer from the surface of the plate, respectively, and they are given by

$$\tau_w = \mu \frac{\partial u}{\partial y}\bigg|_{y=0} , \ q_w = -k_{eff}\left(\frac{\partial T}{\partial y}\right)_{y=0} - \frac{4\sigma}{3K_0}\left(\frac{\partial T^4}{\partial y}\right)_{y=0} . \quad (14)$$

Using equation (8), equation (13) becomes

$$C_f = 2Pe_x^{-1/2} f''(0), \ Nu_x = -\left(1 + \frac{4R_d}{3}\right)Pe_x^{-1/2}\theta'(0). \quad (15)$$

NUMERICAL METHOD AND VALIDATION OF RESULTS

Equations (9) and (10) are nonlinear equations and it is difficult to get a closed form solution for this system of equations. Therefore, these equations subject to the boundary conditions (11) are solved numerically by means of an efficient, iterative, tri-diagonal implicit finite-difference method discussed previously by Blottner (1970).

Equations (9) and (10) are discretized using three-point central difference formulae with f' replaced by another variable V. The η direction is divided into 196 nodal points and a variable step size is used to account for the sharp changes in the variables in the region close to the surface where viscous effects dominate. The initial step size used is $\Delta\eta_1 = 0.001$ and the growth factor $G = 1.037$ such that

$$\Delta\eta_{n^*} = G\Delta\eta_{n^*-1}$$

where the subscript n^* is the number of nodes minus one.

This gives $\eta_{max} \approx 35$ which represents the edge of the boundary layer at infinity. The ordinary differential equations are then converted into linear algebraic equations that are solved by the Thomas algorithm discussed by Blottner (1970). Iteration is employed to deal with the nonlinear nature of the governing equations. The convergence criterion employed in this work was based on the relative difference between the current and the previous iterations. When this difference or error reached 10^{-5}, then the solution was assumed converged and the iteration process was terminated. The accuracy of the numerical method employed in this work is tested by direct comparisons with the previously published work of Gorla et al. (1999) and Cheng and Lin (2007) for special cases of the problem under consideration. Tables 1 - 3 show that excellent agreement between the compared results exists. This lends confidence in the numerical results to be reported subsequently.

RESULTS AND DISCUSSION

In order to get a clear insight on the physics of the problem, a parametric study is performed and the obtained numerical results are displayed with the help of graphical illustrations. The numerical computations were carried out for the fixed values of buoyancy parameter $\Omega=1$ and $\Omega=-1$ which corresponding the aiding and opposing external flows, respectively. The results of this parametric study are shown in Figures 2 - 15.

Velocity and temperature distributions

Figures 2 and 3 show the effect of the melting parameter M on the velocity profiles and temperature distributions for opposing and aiding external flow conditions, respectively. It is seen that there exist a different behavior between the velocity profiles in the presence of solid-phase melting effect in the cases of opposing and aiding flows. This difference is represented in the reduction of the velocity profiles as a result of increasing the melting parameter M for the case of opposing flow whereas the opposite behavior for the velocity fields of the fluid as M increases is predicted for the aiding external flow case. As for the temperature of the liquid, increasing the value of the melting parameter M causes decrease in the temperature distributions for both opposing and aiding flow conditions. A detailed inspection of the temperature profiles show that the temperature distribution for an opposing external flow is higher than that corresponding to aiding external flow under the same conditions. This is related to the presence of buoyancy-assisted force which causes the reduction of the liquid temperature.

The effects of the thermal radiation parameter R_d on the velocity profiles and temperature distributions for the case of opposing external flow and the case of aiding external flow are plotted in Figures 4 and 5. It is evident from these figures that, for opposing external flow conditions, the presence of the thermal radiation affects the activity of the fluid or liquid velocity inversely. This can be seen clearly from the velocity curves which decrease as the radiation parameter R_d increases. For the aiding external flow case, the presence of the radiation leads to increased acceleration of the fluid motion represented by the increase in the liquid velocity. In addition, increasing the values of radiation parameter leads to decreases in the liquid temperature distribution for both cases of opposing and aiding external flow.

Figures 6 and 7 display the effects of the non-Darcy porous medium parameter Re_d on the velocity profiles and temperature distributions for both opposing and aiding flow cases, respectively. These results are interesting because the fluid velocity and temperature take behaviors for opposing flow conditions clearly different from those corresponding to aiding flow conditions. In the opposing flow case, the fluid velocity and temperature increase as the non-Darcy porous medium parameter increases but in the aiding flow case both of the velocity profiles and temperature distributions decrease with increasing values of the non-Darcy porous medium parameter.

Figures 8 and 9 depict the effects of the heat generation or absorption parameter γ on the velocity profiles and temperature distributions for both opposing and aiding external flows, respectively. It is obvious that, for opposing flow conditions, increasing the heat generation or absorption parameter γ has the tendency to increase

Table 1. Comparison of $f''(0)$ with values obtained by Gorla et al. (1999) and Cheng and Lin (2007) for a Newtonian fluid $(n = 1.0)$ with an aiding external flow.

M	Ω	Gorla et al. (1999)	Cheng and Lin (2007)	Present
2.0	0.0	1.000	1.000	1.000
	1.4	2.400	2.400	2.400
	3.0	4.000	4.000	4.000
	8.0	9.000	9.000	9.008
	10.0	11.00	11.00	11.00

Table 2. Comparison of $\theta'(0)$ with values obtained by Gorla et al. [3] and Cheng and Lin [5] for a Newtonian fluid $(n = 1.0)$ with an aiding external flow

M	Ω	Gorla et al. (1999)	Cheng and Lin (2007)	Present
2.0	0.0	0.2799	0.2706	0.2706
	1.4	0.3823	0.3801	0.3802
	3.0	0.4754	0.4745	0.4747
	8.0	0.6902	0.6902	0.6905
	10.0	0.7594	0.7594	0.7598

Table 3. Comparison of $\theta'(0)$ with values obtained by Gorla et al. [3] and Cheng and Lin [5] for a Newtonian fluid $(n = 1.0)$ with an opposing external flow

M	Ω	Gorla et al. (1999)	Cheng and Lin (2007)	Present
0.0	0.2	0.5269	0.5270	0.5272
	0.4	0.4865	0.4866	0.4867
	0.6	0.4420	0.4421	0.4421
	0.8	0.3916	0.3917	0.3917
	1.0	0.3320	0.3321	0.3320
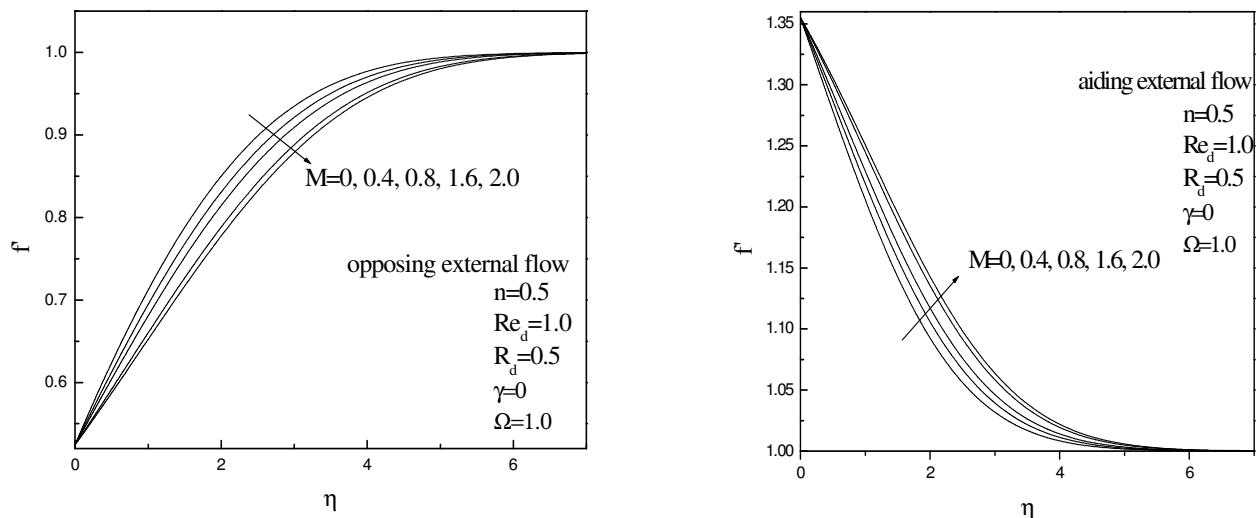
Figure 2. Effects of melting parameter on velocity profiles.
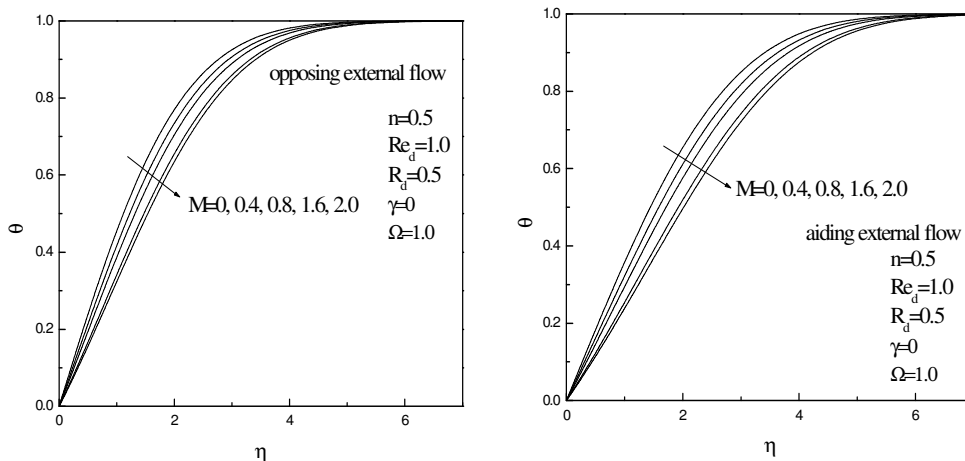
Figure 3. Effects of melting parameter on temperature profiles.
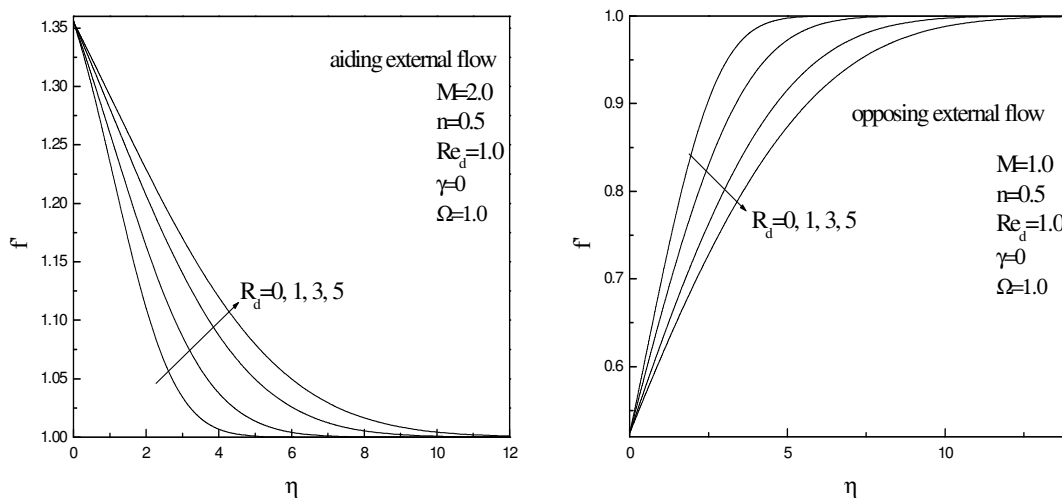
Figure 4. Effect of radiation parameter on velocity profiles.
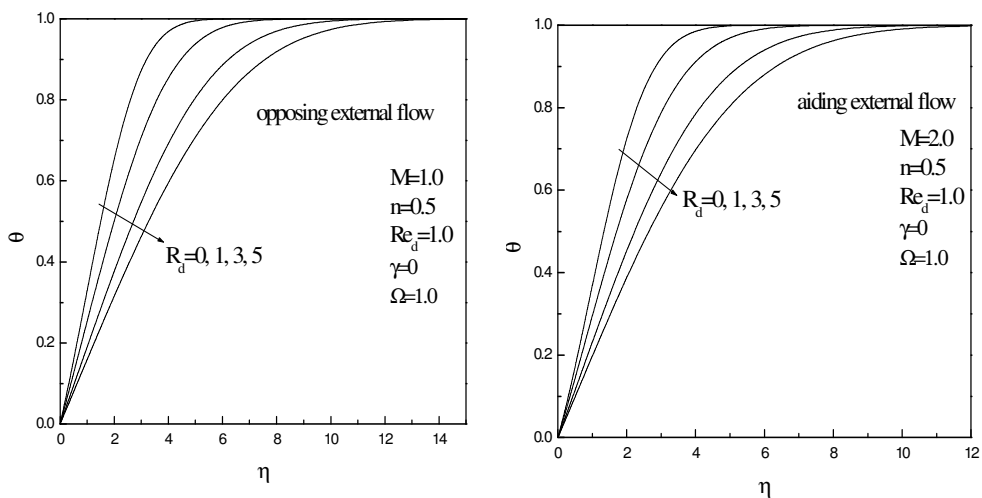
Figure 5. Effect of radiation parameter on temperature profiles.
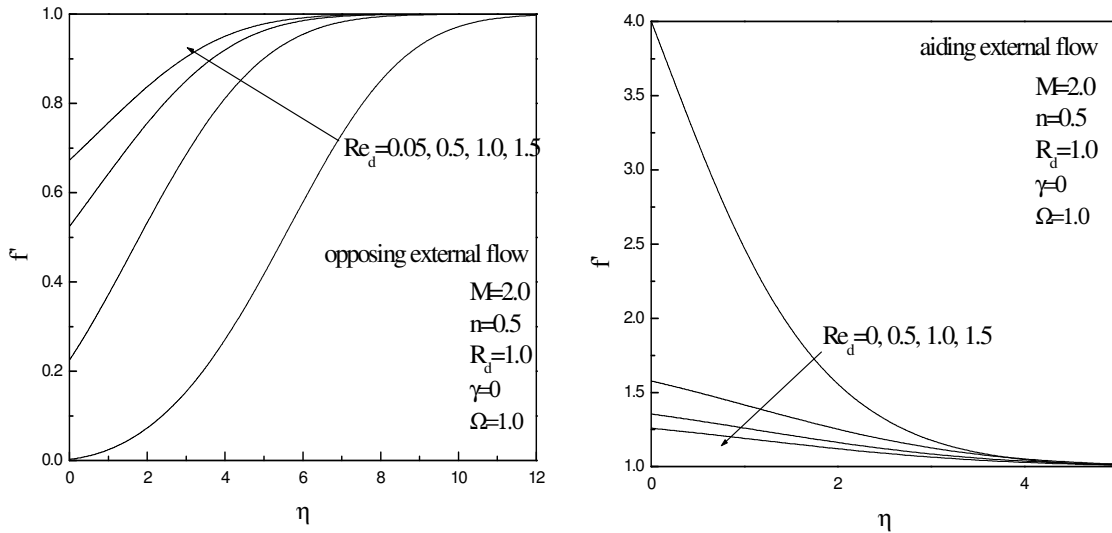
Figure 6. Effect of non-Darcy porous medium parameter on velocity profiles.
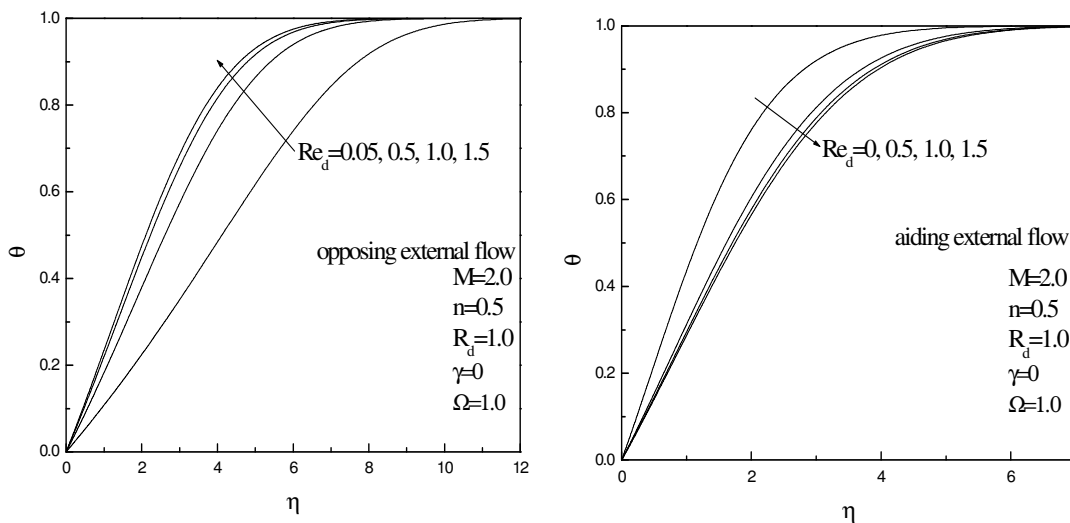
Figure 7. Effect of non-Darcy porous medium parameter on temperature profiles.

increase the liquid temperature which in turn causes an increased induced flow along the plate due to buoyancy effect. This is represented by the increased fluid velocity as γ increases. On the other hand, for aiding flow conditions, while the presence of a heat source leads to increases in the liquid temperature, the velocity of the liquid decreases due to the change in sign of the buoyancy term in the momentum equation. The opposite behaviors take place due to the presence of a heat sink.

Figures 10 and 11 present the effects of fluid viscosity index n on the fluid velocity and temperature distributions for opposing and aiding external flow conditions, respectively. It is clear from these figures that, increasing the fluid viscosity index n causes decreases in the velocity of the fluid and increases in its temperature for the opposing flow case while the opposite behavior is predicted for the aiding flow case namely; increases in the liquid velocity and decreases in its temperature. Note that, the effect of the fluid viscosity index n appears to be more pronounced for aiding flow than for opposing flow conditions. These behaviors are clearly seen in Figures 10 and 11.

Skin-friction coefficient and Nusselt number

Figures 12 and 13 illustrate the effects of the radiation parameter R_d and the melting parameter M on the skin-
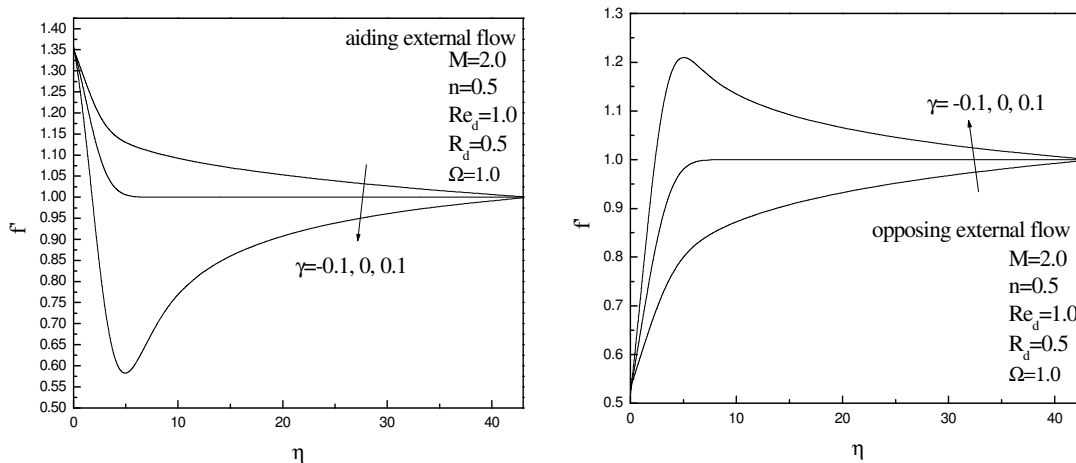
Figure 8. Effect of heat generation or absorption parameter on velocity profiles.
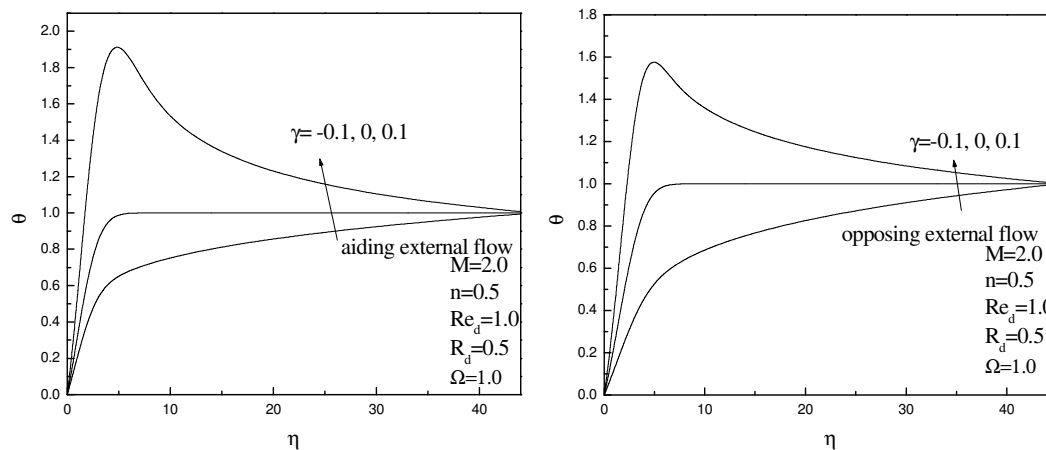
Figure 9. Effect of heat generation or absorption parameter on temperature profiles.
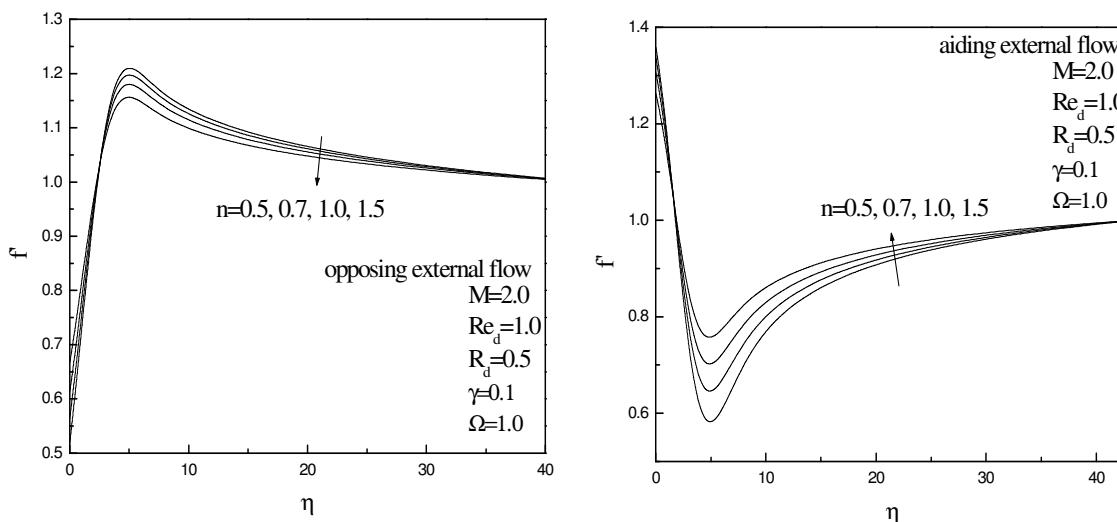
Figure 10. Effect of power-law fluid viscosity index on velocity profiles.
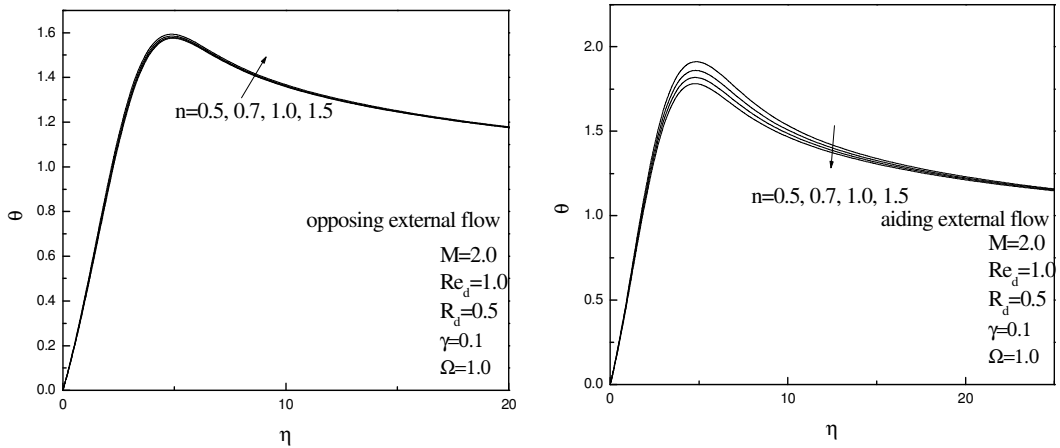
Figure 11. Effect of power-law fluid viscosity index on temperature profiles.
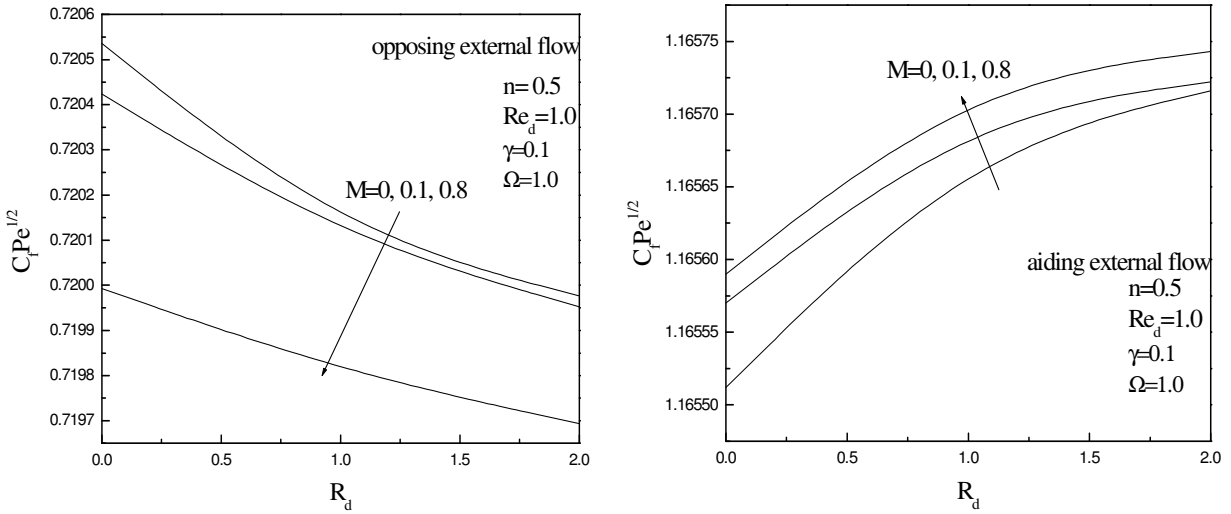
Figure 12. Effect of radiation parameter on skin-friction coefficient for different values of melting parameter.
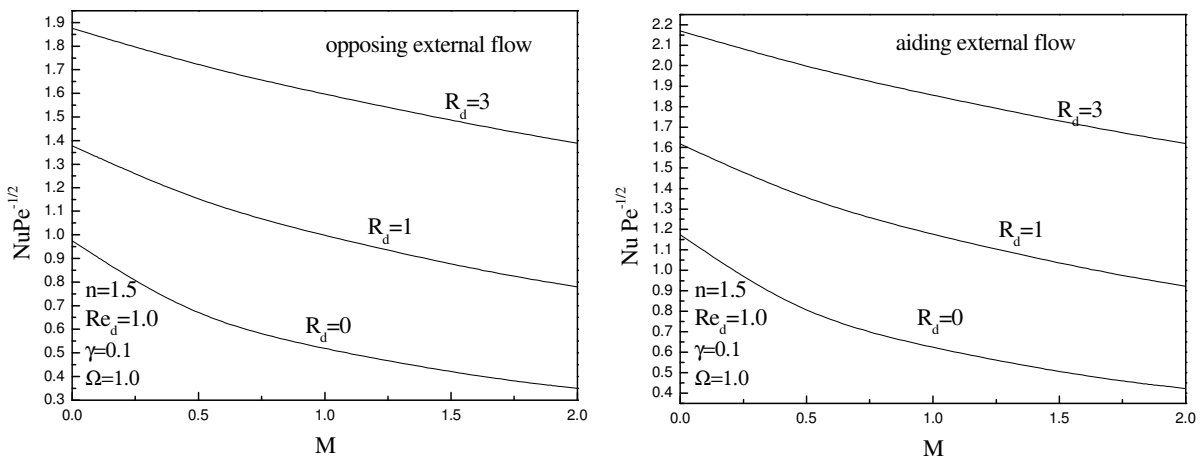
Figure 13. Effect of radiation parameter on Nusselt number for different values of melting parameter.
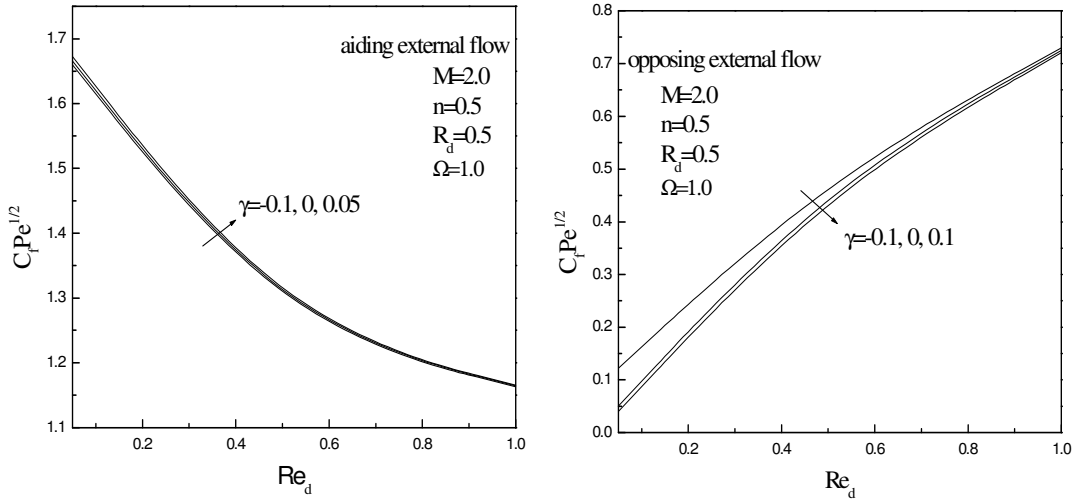
Figure 14. Effect of heat generation or absorption parameter on skin-friction coefficient for different values of non-Darcy porous medium parameter.
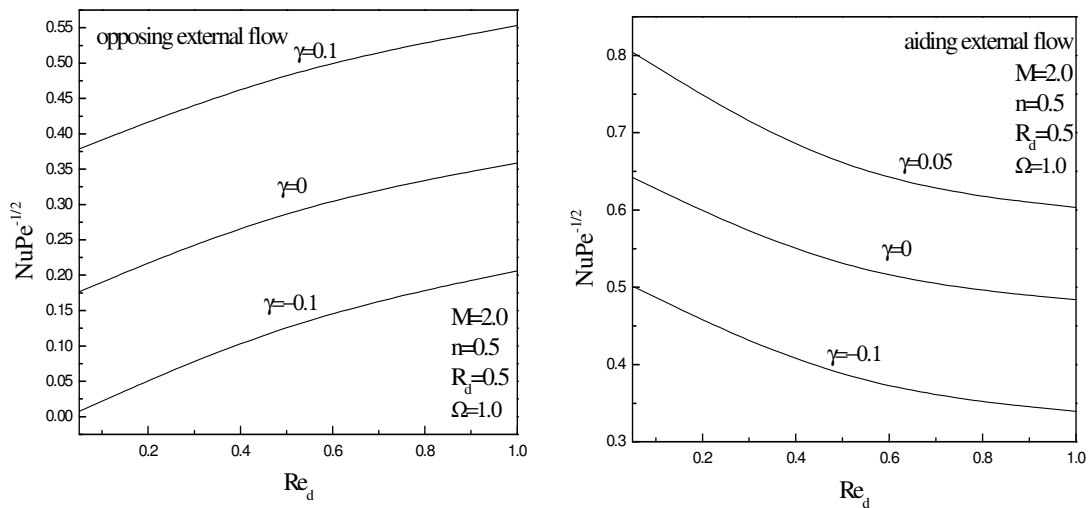
Figure 15. Effect of heat generation or absorption parameter on Nusselt number for different values of non-Darcy porous medium parameter.

friction coefficient $C_f Pe_x^{1/2}$ and the Nusselt number $Nu_x Pe_x^{-1/2}$ for the cases of opposing and aiding external flows, respectively. It is clear that, for opposing flow conditions, increasing the values of the radiation parameter R_d and the melting parameter M causes the skin-friction coefficient $C_f Pe_x^{1/2}$ to decrease. For the aiding flow case, the skin friction coefficient $C_f Pe_x^{1/2}$ increases with increases in either of the melting parameter M or the radiation parameter R_d. Regarding the Nusselt number $Nu_x Pe_x^{-1/2}$, for the opposing flow, increasing the values of the melting parameter M yields

decreases in the Nusselt number $Nu_x Pe_x^{-1/2}$ whereas it increases due to increases in the radiation parameter R_d. For aiding flow condition, the same behaviors as those of the opposing flow case are observed. Figures 14 and 15 depict the effects of the heat generation or absorption parameter γ and non-Darcy porous medium parameter Re_d on the skin-friction coefficient $C_f Pe_x^{1/2}$ and the Nusselt number $Nu_x Pe_x^{-1/2}$ for the cases of opposing and aiding external flows, respectively. It is predicted that, for the case of opposing external flow, increasing the value of the heat generation or absorption parameter γ causes decreases in the skin-friction coeffi-

cient $C_f Pe_x^{1/2}$ and increases in the Nusselt number $Nu_x Pe_x^{-1/2}$ whereas, increasing the value of non-Darcy porous medium parameter Re_d results in increasing not only the skin-friction coefficient $C_f Pe_x^{1/2}$ but the Nusselt number $Nu_x Pe_x^{-1/2}$ as well.

However, for the case of aiding external flow, the exact opposite behaviors in the skin-friction coefficient are predicted whereas the Nusselt number increases as the non-Darcy porous medium parameter increases for opposing external flow while it decreases for aiding external flow as clearly seen from Figures 14 and 15.

CONCLUSION

The problem of mixed convection from a vertical surface embedded in a non-Newtonian power-law fluid saturated non-Darcy porous medium in the presence of melting, radiation and heat generation or absorption effects for aiding and opposing external flows was studied. The governing equations were developed and transformed into a self-similar form. The similarity equations were solved numerically by an efficient, tri-diagonal, implicit finite-difference method. From the results of the problem, it was observed that:

(1) Increasing the value of the melting parameter resulted in decreases in the velocity profiles for opposing external flow and increases in the velocity profiles for aiding external flow but in both cases, the temperature distributions decreased.
(2) The presence of thermal radiation decreased the liquid velocity for opposing external flow and increased it for aiding external flow.
(3) The presence of internal heat generation caused increases in the liquid velocity for opposing external flow while the opposite behavior is observed for aiding external flow. In both cases, the liquid temperature increased.
(4) For the opposing flow case, the skin-friction coefficient decreased as either of the melting parameter or the radiation parameter increased whereas the opposite behavior is predicted for the aiding flow case.
(5) Increasing the heat generation or absorption parameter resulted in decreases in the skin-friction coefficient for opposing external flow and increases in its value for aiding external flow.
(6) The Nusselt number decreased as the melting parameter increased while it increased as the radiation parameter increased.
(7) Increasing the heat generation or absorption parameter resulted in increases in the Nusselt number for both opposing and aiding external flows. The Nusselt number also increased as the non-Darcy porous medium parameter increased for opposing external flow while it decreased for aiding external flow.

REFERENCES

Afify AA (2007). Effects of variable viscosity on non- Darcy MHD free convection along a non-isothermal vertical surface in a thermally stratified porous medium, Appl. Math. Modell. 31: 1621–1634.

Ali ME (2007). The effect of lateral mass flux on the natural convection boundary layers induced by a heated vertical plate embedded in a saturated porous medium with internal heat generation, Int. J. Therm. Sci. 46: 157–163.

Bakier AY (1997). Aiding and opposing mixed convection flow in melting from a vertical flat plate embedded in a porous medium, Transport in Porous Media 29: 127–139.

Bakier AY, Rashad AM, Mansour MA (2009). Group method analysis of melting effect on MHD mixed convection flow from radiate vertical plate embedded in a saturated porous media, Commun. Nonlinear Sci. Numer. Simulat. 14: 2160–2170.

Blottner FG (1970). Finite-difference methods of solution of the boundary-layer equations, AIAA J. 8: 193-205.

Chamkha AJ (1996). Non-Darcy hydromagnetic free convection from a cone and a wedge in porous media, Int. Comm. Heat Mass Transfer 23: 875-887.

Chamkha AJ, Al-Mudhaf AF, Pop I (2006). Effect of heat generation or absorption on thermophoretic free convection boundary layer from a vertical flat plate embedded in a porous medium, Int. Comm. Heat Mass Transfer 33: 1096–1102.

Chang WJ, Yang DF (1996). Natural convection for the melting of ice in porous media in a rectangular enclosure, Int. J. Heat Mass Transfer 39: 2333–2348.

Chen MM, Farhadieh R, Baker Jr L (1986). On free convection melting of a solid immersed in a hot dissimilar fluid, Int. J. Heat Mass Transfer 29: 1087–1093.

Cheng C (2008). Double-diffusive natural convection along a vertical wavy truncated cone in non-Newtonian fluid saturated porous media with thermal and mass stratification, Int. Commun. Heat Mass Transfer 35: 985–990.

Cheng WT, Lin CH (2006). Transient mixed convective heat transfer with melting effect from the vertical plate in a liquid saturated porous medium, Int. J. Engrng. Sci. 44: 1023–1036.

Cheng WT, Lin CH (2007). Melting effect on mixed convection heat transfer with aiding and opposing flows from the vertical plate in a liquid saturated porous medium, Int. J. Heat Mass Transfer 50: 3026–3034.

Cheng WT, Lin CH (2008). Unsteady mass transfer in mixed convective heat flow from a vertical plate embedded in a liquid-saturated porous medium with melting effect, Int. Commun. Heat Mass Transfer 35: 1350–1354.

Degan G, Akowanou C, Awanou NC (2007). Transient natural convection of non-Newtonian fluids about a vertical surface embedded in an anisotropic porous medium Int. J. Heat Mass Transfer 50: 4629-4639.

Epstein M, Cho DH (1976). Laminar film condensation on a vertical melting surface, ASMEJ. Heat Transfer 98: 108–113.

Gorla RSR, Mansour MA, Hassanien IA, Bakier AY (1999). Mixed convection effect on melting from a vertical plate, Transport in Porous Media 36: 245–254.

Hassanien IA, Al-arabi TH (2009). Non–Darcy unsteady mixed convection flow near the stagnation point on a heated vertical surface embedded in a porous medium with thermal radiation and variable viscosity, Commun. Nonlinear. Sci. Numer. Simulat. 14: 1366–1376.

Kazmierczak M, Poulikakos D, Pop I (1986). Melting from a flat plate embedded in a porous medium in the presence of steady natural convection, Numer. Heat Transfer 10: 571–581.

Kazmierczak M, Poulikakos D, Sadowski D (1987). Melting of a vertical plate in porous medium controlled by forced convection of a dissimilar fluid, Int. Comm. Heat Mass Transfer 14: 507–517.

Kumari M, Nath G (2006). Conjugate mixed convection transport from a moving vertical plate in a non-Newtonian fluid, Int. J. Therm. Sci. 45: 607–614.

Murthy PVSN, Mukherjee S, Kharagpur D, Srinivasacharya PVS, Krishna SSR (2004). Combined radiation and mixed convection from a vertical wall with suction/injection in a non–Darcy porous medium, Acta Mech. 168: 145–156.

Murthy PVSN, Singh P (2000). Thermal dispersion effects on non-Darcy convection over a cone, Comp. Math. with Applications 40: 1433-1444.

Poulikakos D, Spatz TL (1988). Non-Newtonian natural convection at a melting front in a permeable solid matrix, Int. Commun. Heat Mass Transfer 15: 593–603.

Rastogi SK, Poulikakos D (1995). Double-diffusion from a vertical surface in a porous region saturated with a non-Newtonian fluid, Int. J. Heat Mass Transfer 38: 935–946.

Roberts L (1958). On the melting of a semi-infinite body of ice placed in a hot stream of air, J. Fluid Mech. 4: 505–528.

Sparrow EM, Patankar SV, Ramadhyani S (1977). Analysis of melting in the presence of natural convection in the melt region, ASME J. Heat Transfer 99: 520–526.

Tashtoush B (2005). Magnetic and buoyancy effects on melting from a vertical plate embedded in saturated porous media, Energy Conversion and Management 46: 2566–2577.

Tien C, Yen YC (1965). The effect of melting on forced convection heat transfer, J. Appl. Meteorol. 523–527.

Walker G (2007). A world melting from the top down, Nature 446: 718–721.

Zhang Z, Bejan A (1989). The problem of time-dependent natural convection melting with conduction in the solid, Int. J. Heat Mass Transfer 32: 2447–2457.